

## Title Page

### **Retinal transcriptome and cellular landscape in relation to the progression of diabetic retinopathy**

Jiang-Hui Wang, PhD<sup>1,2\*</sup>; Raymond C.B. Wong, PhD<sup>1,2</sup>; Guei-Sheung Liu, PhD<sup>1,2,3,4\*</sup>

<sup>1</sup>Centre for Eye Research Australia, Royal Victorian Eye and Ear Hospital, East Melbourne, Australia

<sup>2</sup>Ophthalmology, Department of Surgery, University of Melbourne, East Melbourne, Victoria, Australia

<sup>3</sup> Menzies Institute for Medical Research, University of Tasmania, Hobart, Australia

<sup>4</sup>Aier Eye Institute, Changsha, Hunan, China

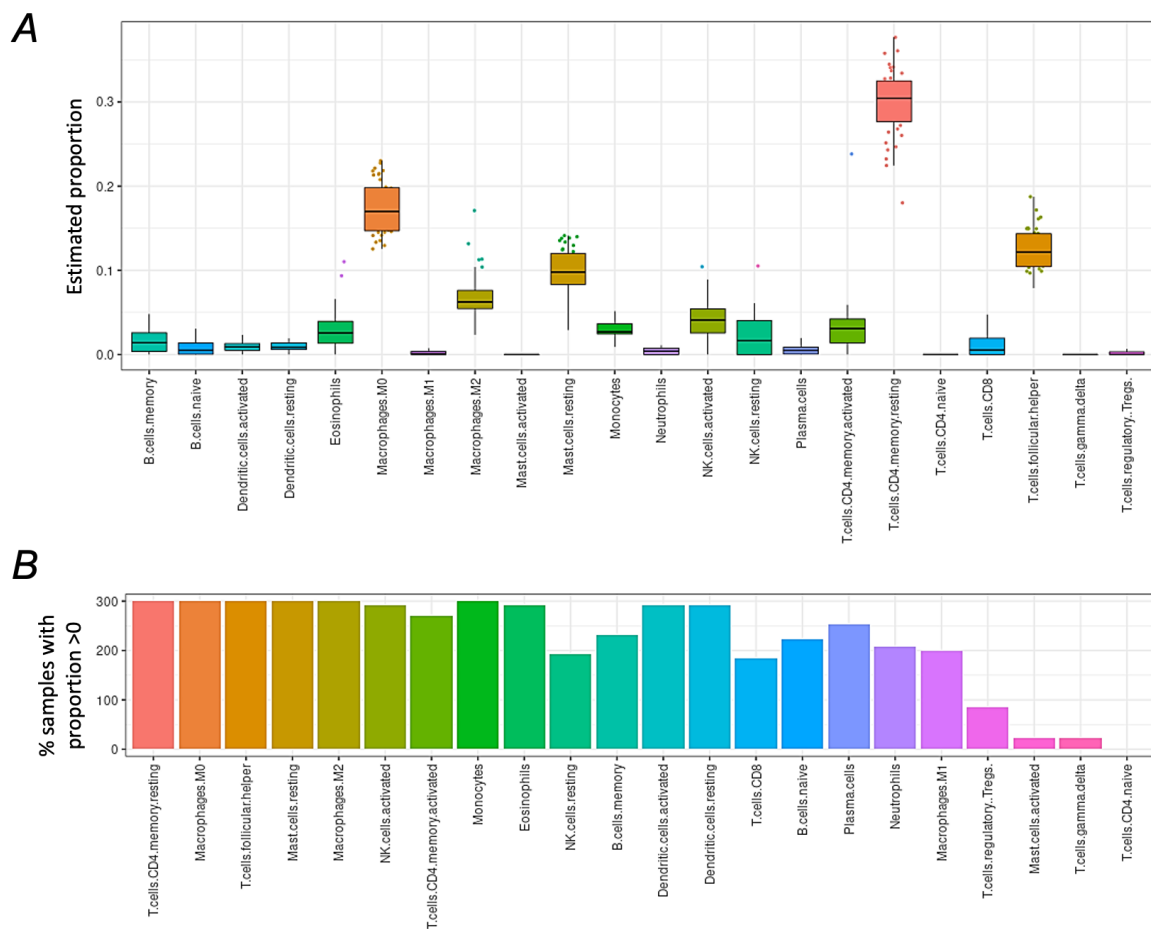
\*Correspondence and requests for materials should be addressed to

Dr Jiang-Hui Wang (sloanjhwang@gmail.com). Centre for Eye Research Australia. Address: Level 7, 32 Gisborne Street, East Melbourne, VIC 3002, Australia. Tel: +61399298463.

Or

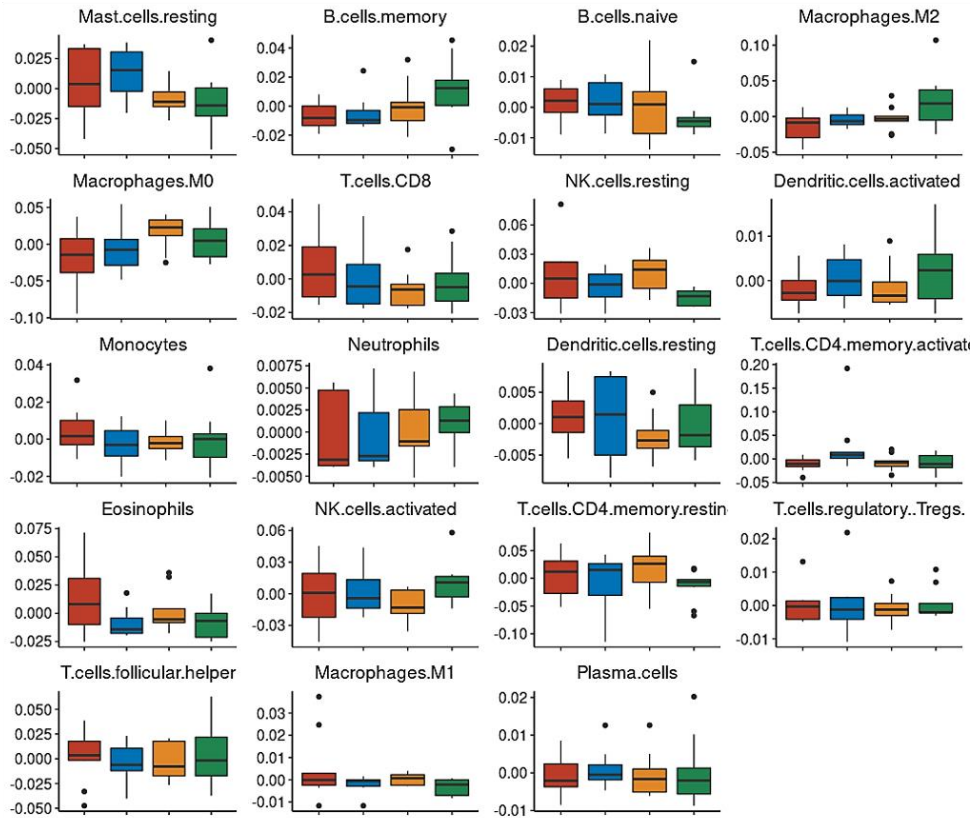
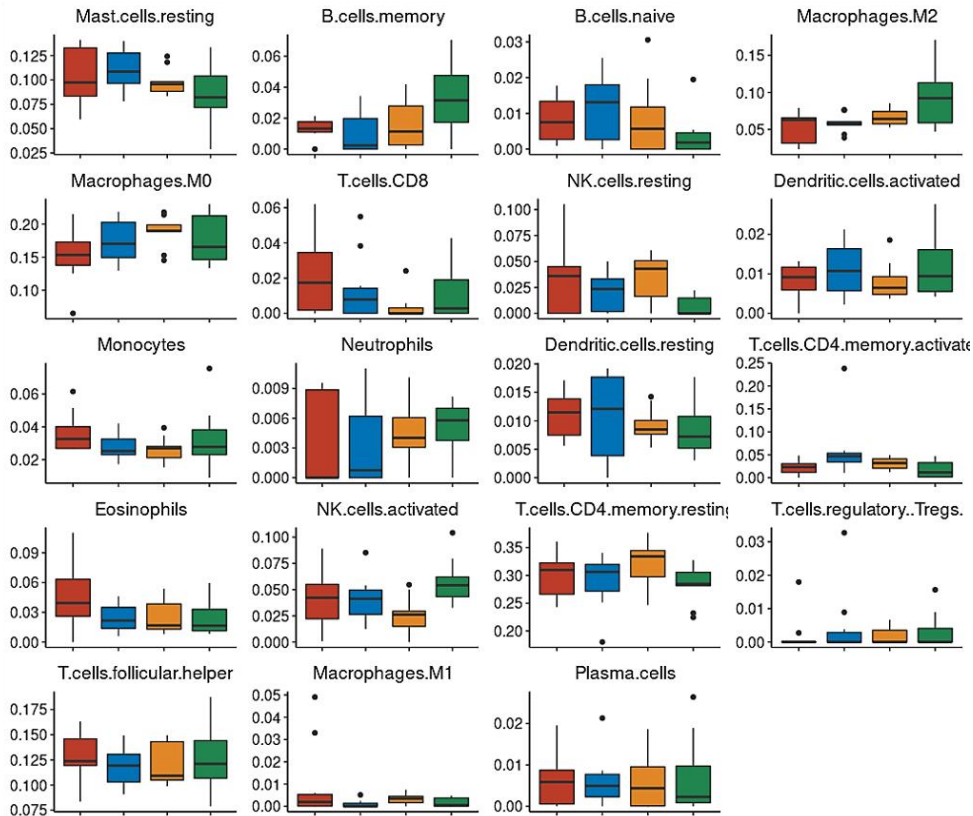
Dr Guei-Sheung Liu (rickliu0817@gmail.com). Centre for Eye Research Australia. Address: Level 7, 32 Gisborne Street, East Melbourne, VIC 3002, Australia. Tel: +61362264250.

## Supplementary Figures

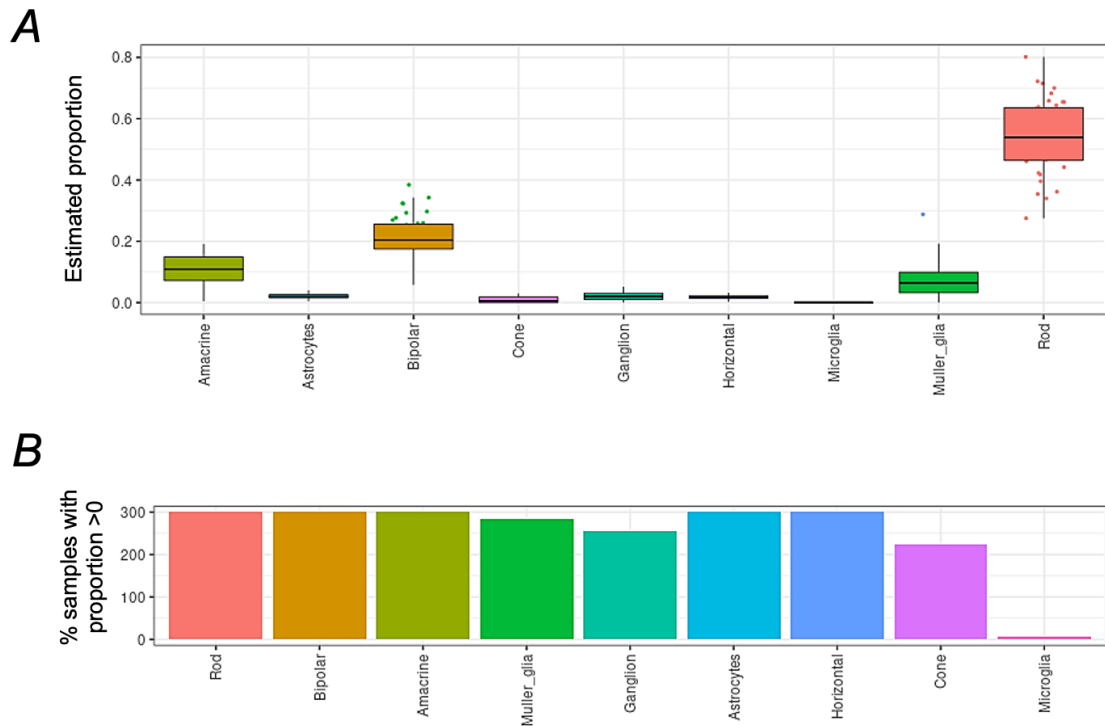


### Supplementary Fig. 1. General information of deconvolution analyses for immune cells.

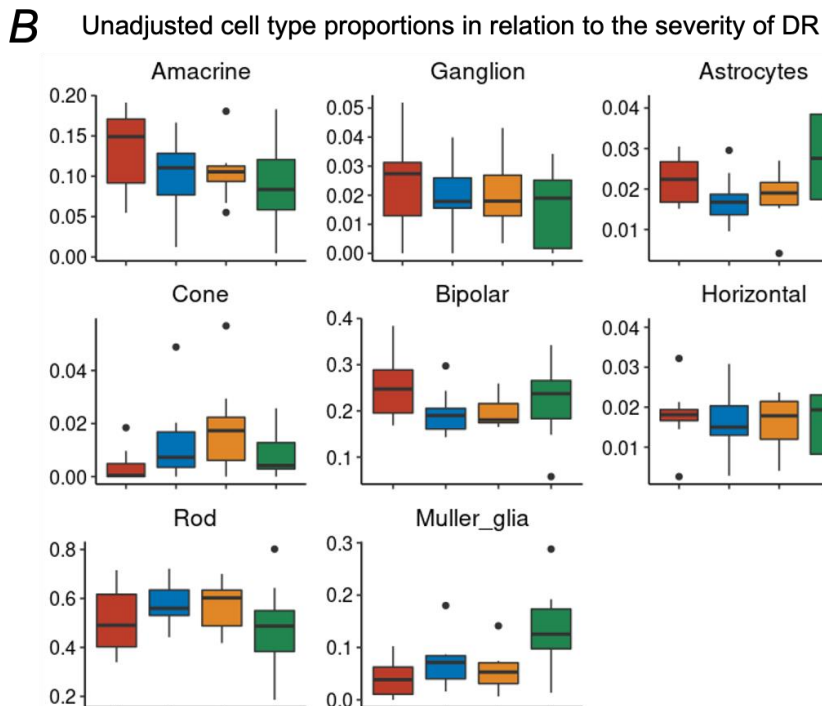
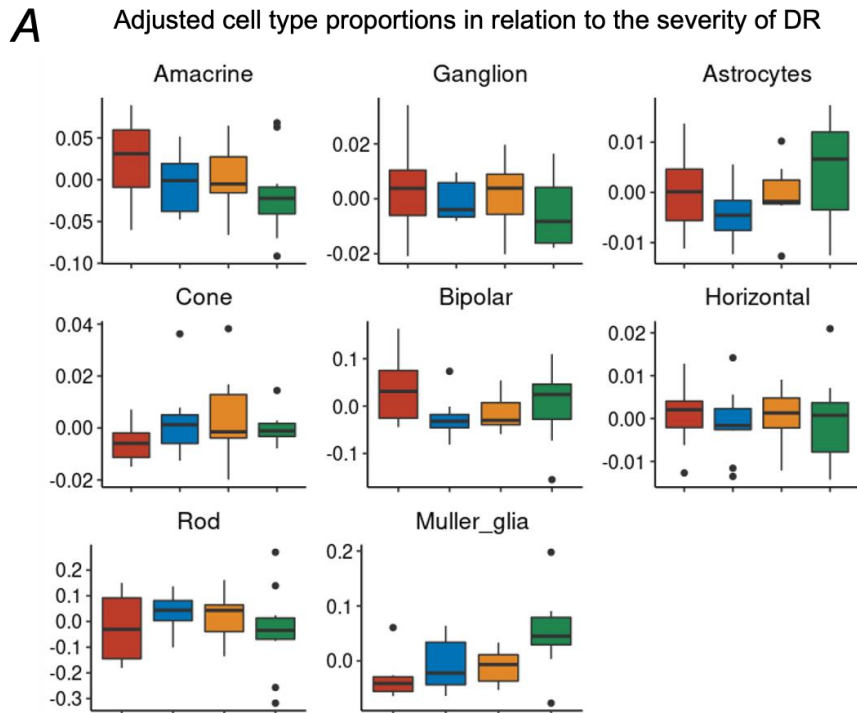
A. Tukey boxplots (interquartile range (IQR) boxes with  $1.5 \times \text{IQR}$  whiskers) showing the estimated proportions of immune cell types across all samples ( $n=39$ ), as estimated by deconvolution analyses with CIBERSORTx (22 immune cell types). B. Bar plot indicating the percentage of samples with non-zero estimated proportions for each immune cell type ( $n = 39$ ).

**A****Adjusted cell type proportions in relation to the severity of DR****B****Unadjusted cell type proportions in relation to the severity of DR**

**Supplementary Fig. 2. Adjusted and unadjusted proportions of immune cell types in relation to the severity of DR.** A and B. Tukey boxplots (interquartile range (IQR) boxes with  $1.5 \times \text{IQR}$  whiskers) showing the adjusted or unadjusted estimated proportions of each immune cell type across different degree of DR ( $n = 39$ ). The proportions estimated by CIBERSORTx were adjusted for gender and age.



**Supplementary Fig. 3. General information of deconvolution analyses for retinal cells.** A. Tukey boxplots (interquartile range (IQR) boxes with  $1.5 \times \text{IQR}$  whiskers) showing the estimated proportions of retinal cell types across all samples ( $n=39$ ), as estimated by deconvolution analyses with CIBERSORTx (22 immune cell types). B. Bar plot indicating the percentage of samples with non-zero estimated proportions for each retinal cell type ( $n = 39$ ).



**Supplementary Fig. 4. Adjusted and unadjusted proportions of retinal cell types in relation to the severity of DR.** A and B. Tukey boxplots (interquartile range (IQR) boxes with  $1.5 \times$  IQR whiskers) showing the adjusted or unadjusted estimated proportions of each retinal cell type across different degree of DR ( $n = 39$ ). The proportions estimated by CIBERSORTx were adjusted for gender and age.